as shown in Fig. 2.12. Various characteristics of these capacitors were measured and are presented in Section 2.1.3.

Fig. 2.9. Comparison of all capacitors located within Camry PCU.

Fig. 2.10. Cutaway of dc-link capacitor removed from shell (left) and x-ray of module (right).

Fig. 2.11. Battery level capacitor (upper) and x-ray of module (lower).

Fig. 2.12. Small dc-link capacitor: overhead view (left) and x-ray of module – side view (lower).

Figure 2.13 shows a view of the inverter/converter assembly upside down with the three-phase motor and generator bus connector assembly unbolted and detached. It can be seen that CTs are used on two of the three bus connectors. The red rubber seal inserts into the inverter housing in order to facilitate a sealed union. In general, the inverter and converter housings are very well sealed and are water tight to prevent contamination and corrosion from environmental effects.

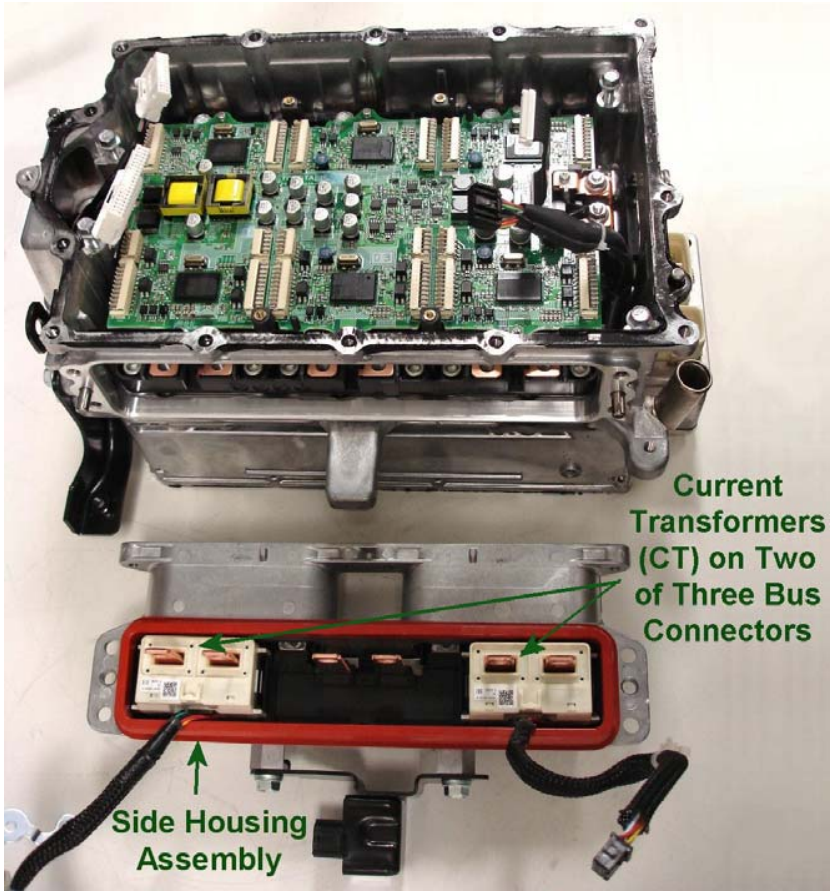

Fig. 2.13. Side housing removed from inverter section of PCU (shown upside down).

2.1.1 Power Electronics Devices

The general packaging features of the Camry inverter and converter power electronic devices were assessed and compared to the Prius designs. Figure 2.14 shows a comparison between the Camry and the Prius IPMs which were photographed while sitting adjacent to each other. All power electronic devices shown are immersed in a high-temperature, protective silicone gel. Although the power capability of the IPM increases from the Prius to the Camry, the size of the IPM noticeably decreases. The general layout of the IPM design is similar, wherein the shared dc bus, indicated by the red line, runs between the motor and generator inverters. However, a closer inspection yields several differences between the two. Bus bars are used to interconnect the dc link and phase outputs to the power electronics devices of the Prius IPM, yet the Camry IPM does not use a conventional bus bar architecture to accomplish this task. Instead, a more interweaved layout is used which enhances the area utilization of the IPM. The Camry IPM layout allows for the space below the dc-bus bars to be used as extra surface area for power electronics devices, as shown in Fig. 2.15. It can also be noticed that there is enough space for the Camry generator inverter to contain twice the number of IGBTs than what is currently present. Toyota has made an effort to standardize the size of the PCU and this space is likely utilized in HEVs with larger power trains, such as the Toyota Highlander HEV or the Lexus GS450h. The maximum power supplied to the motor inverter must be less than (due to losses) the sum of the battery power and the generator power. It is likely that the full capability of the motor inverter is not fully utilized in the vehicle, as the generator inverter can supply only 1/3 of the power capability to the motor inverter and any additional power must be supplied by the battery which has a power rating of 30 kW, and the combined peak power is approximately 70 kW.

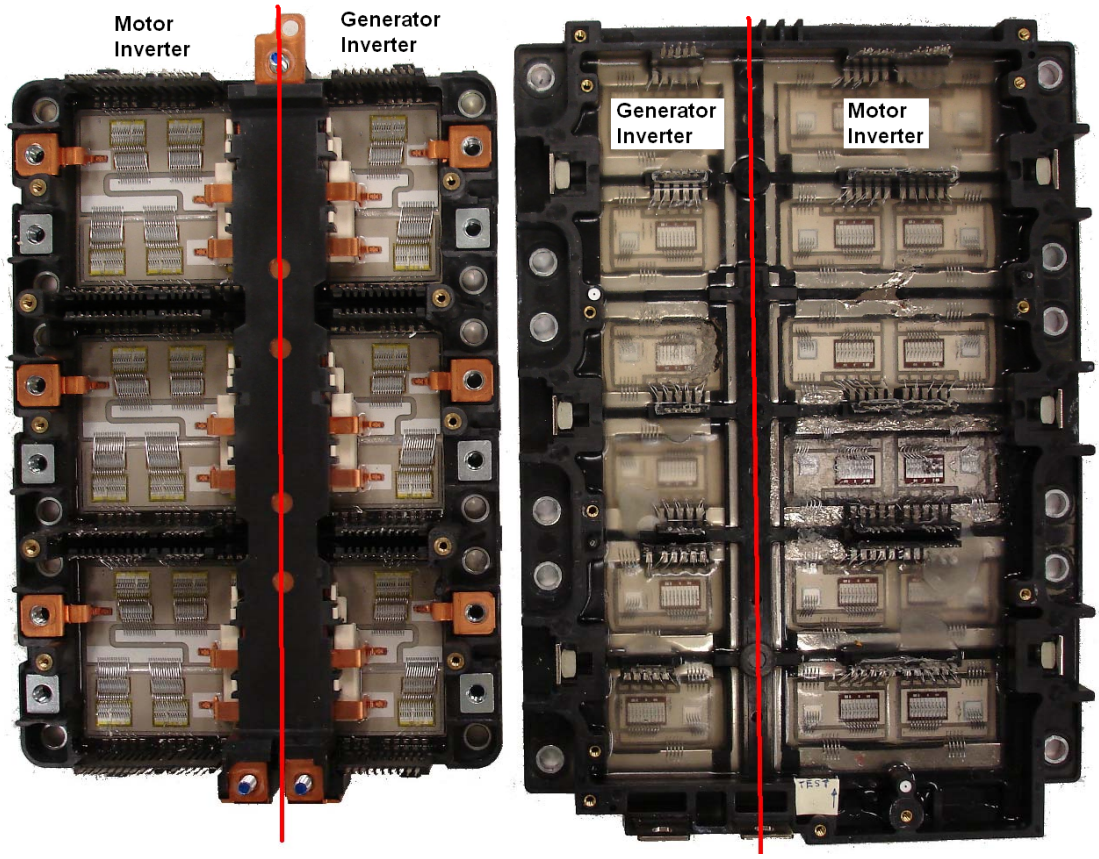

Fig. 2.14. Comparison of Camry inverter IPM (left) and Prius inverter IPM (right).

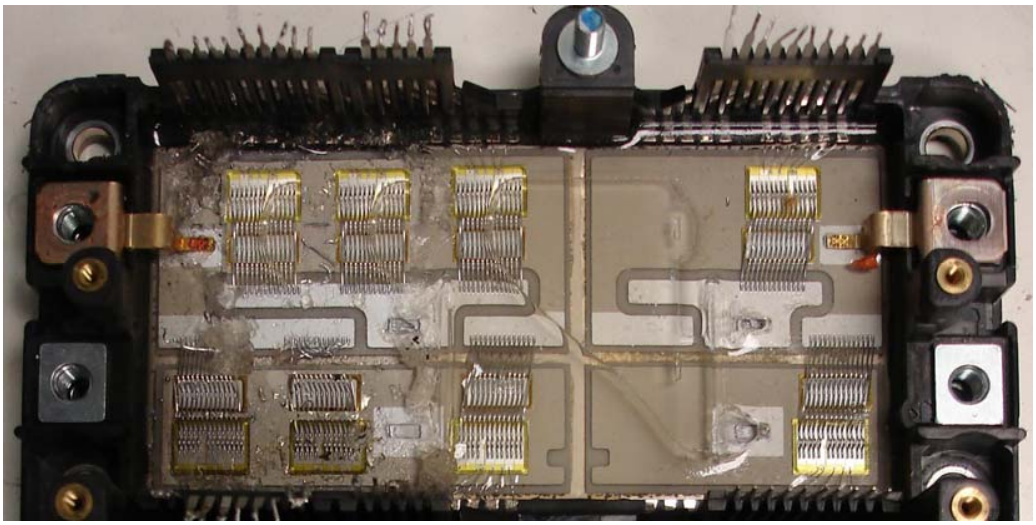

Fig. 2.15. Camry IPM with dc-bus bars removed.

Figure 2.16 provides a more detailed representation of the design discrepancies as well as a dimensional comparison of the IGBTs and diodes of the Camry and Prius inverter power electronics. Since the emitters and collectors of the Camry IPM are not connected to bus bars as they are in the Prius, additional room is available for situating the diodes in an orientation which is more efficient in terms of surface area

utilization. In the Prius inverter image shown in Fig. 2.16, the IGBT emitter and diode anode are tied to a common metal plate, which is connected to a bus bar that is partially visible on the left edge of the image. The IGBT collector and diode cathode are connected to a bar which is just beyond the right edge of the image. Conversely, the Camry dc link and three-phase outputs connect directly to the emitter-anode common plate and the collector-cathode surface, thereby eliminating the use of a bus bar infrastructure.

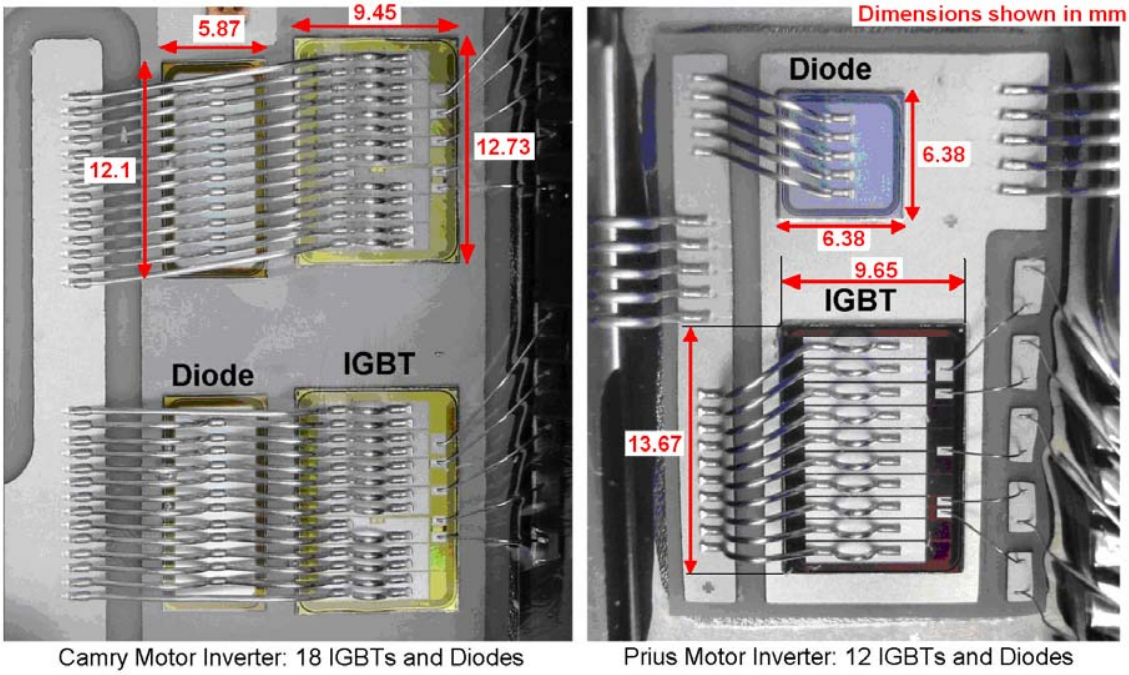

Fig. 2.16. Dimensions (in mm) of Camry inverter IPM (left) and Prius inverter IPM (right).

As indicated by the labeled dimensions, the Camry inverter IGBT size has decreased from the Prius inverter IGBT size in both length and width, whereas the size of the diode increased significantly. Although the Camry IGBT chip size has decreased when compared to that of the Prius IGBT, the power capability has increased slightly. This is primarily due to the use of a trench gate structure as opposed to the planar gate structure used in the Prius. The planar gate structure includes areas in the drift region below the emitter "n+" and "p" regions which do not pass as much current as the drift region areas below the gate. This inefficiency is due to the shape of the inversion layer which is formed when using a planar gate structure. An IGBT with a trench gate structure forms a more uniform inversion layer during on-state operation, and therefore higher current densities are created in the drift region. Additionally, the voltage rating of the Camry IGBT devices has increased, facilitating higher power capability and higher power density of the generator, motor, and the respective inverters.

A detailed comparison of the Camry and Prius IGBTs is shown in Fig. 2.17. The Camry IGBT contains two wire bonds for each emitter strip, whereas the Prius only has one wire bond for each emitter strip. Both IGBTs include leads for semiconductor junction temperature measurement feedback, gate voltage control, current measurement, and emitter voltage feedback. These signals are used to control the device and prevent fault conditions from occurring. Cross-sectional views of the IGBTs are provided in Fig. 2.18. Small metallic nodes are visible on the Camry IGBT, yet there is no evidence of these nodes on the Prius IGBT. These nodes are likely associated with the trench gate structure, but are not directly associated with the trench pitch as the metal nodes are separated by about 20 μm, which is much larger than typical trench pitches.

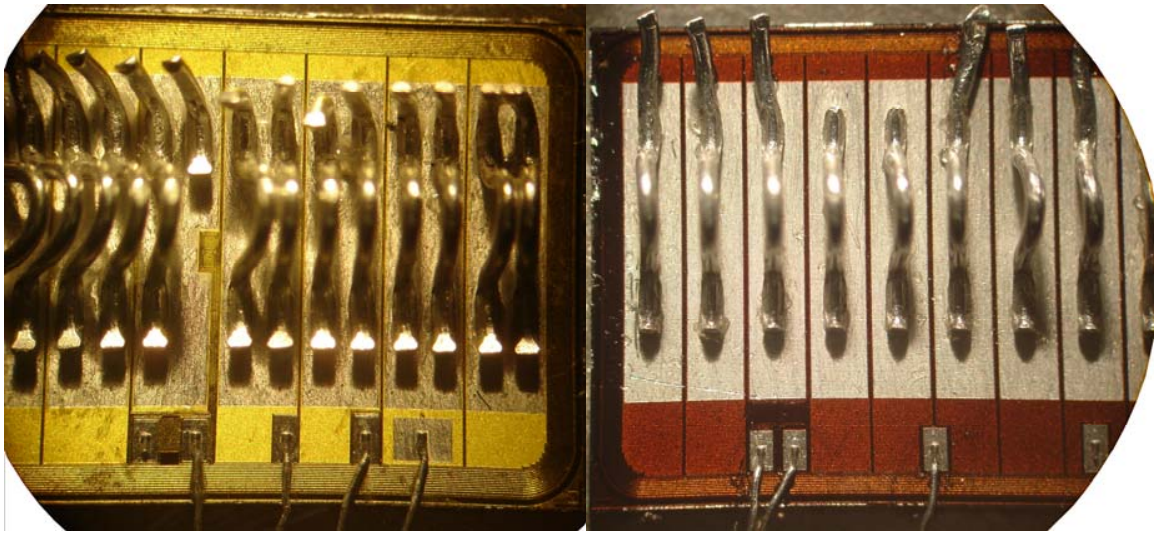

Fig. 2.17. Close-up view of Camry inverter IGBT (left) and Prius inverter IGBT (right).

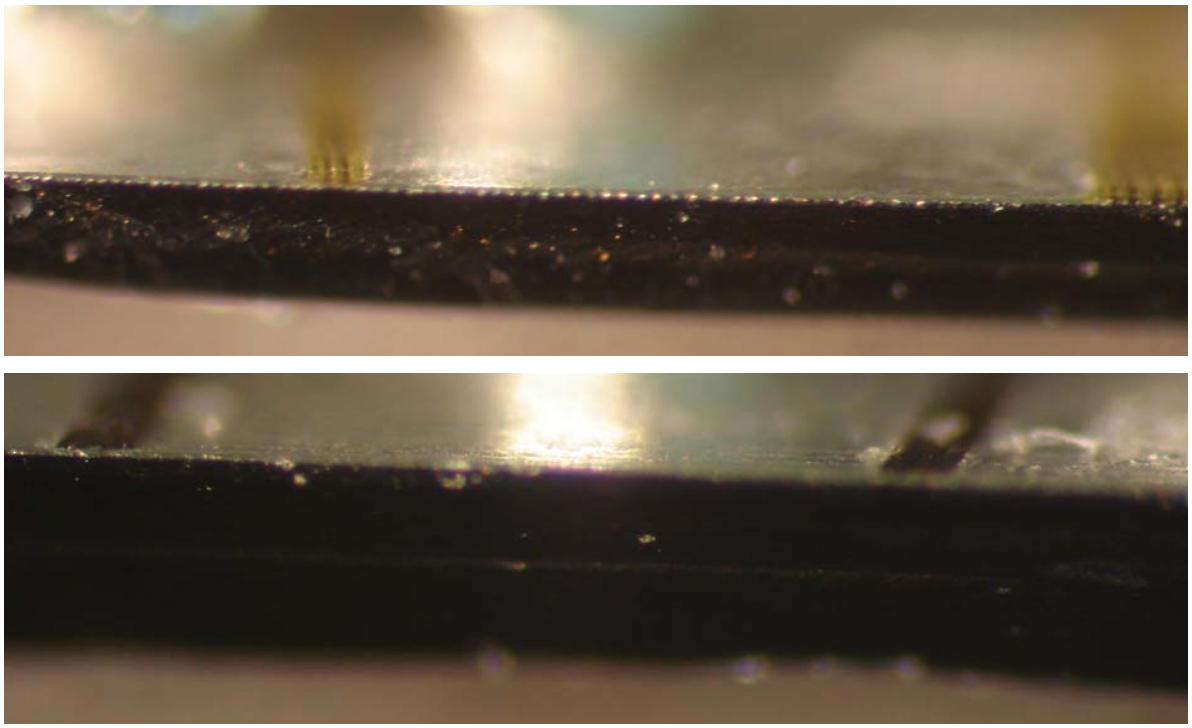

Fig. 2.18. Cross-sectional view of Camry IGBT (upper) and Prius IGBT (lower).

Diodes from the Camry and Prius inverters are shown in Fig. 2.19. The shape of the Camry inverter diode is elongated providing well-suited orientation with the adjacent IGBT. Several traces are located around the perimeter of the Camry and Prius diodes and IGBTs, which is possibly a preventative measure against catastrophic arcing.

Fig. 2.19. Close-up view of Camry inverter diode (left) and Prius inverter diode (right).

The Camry and Prius boost converter IPMs are shown in Fig. 2.20. Although the power rating of the boost converter has increased by 50% from the Prius, the area of the Camry boost converter IPM footprint is only slightly larger than that of the Prius. Similar to the discrepancies between the inverters, smaller bus architecture is used in the Camry boost converter IPM. There is a considerably larger amount of null space within the Prius boost converter module. The Camry boost converter has four IGBTs and diodes in parallel for the upper portion of the IPM and four IGBTs and diodes in parallel for the lower portion of the IPM. The four upper IGBTs and four lower diodes are primarily used during regenerative braking and recharging situations. The four lower IGBTs and four upper diodes are primarily used to boost the battery voltage. The Prius boost converter IPM is similar in functionality, but has only two IGBTs and two diodes in parallel for the upper and lower portions. The Prius boost converter IPM also only has three terminals versus six on the Camry IPM, four of which are used to conduct power. The upper-left terminal does not connect to the IPM, but serves as a support for the negative dc-link bus bar and capacitor connection. The lower-left terminal serves as a support for the positive dc-link bus bar (which connects to the inductor) and capacitor connection, and through a small wire it is connected to a pin which interfaces with the IPM driver-board.

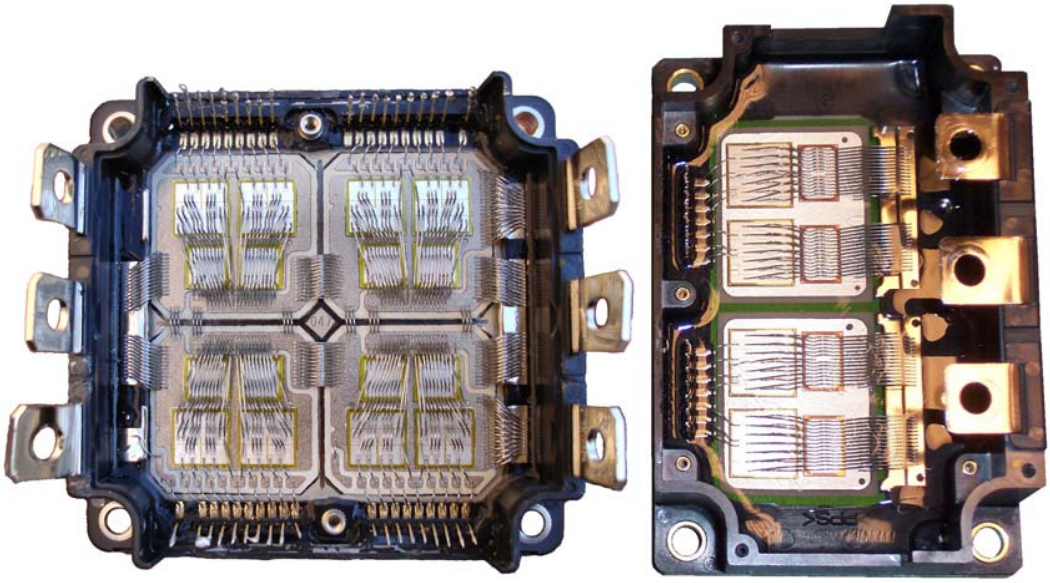

Fig. 2.20. Comparison of Camry converter IPM (left) and Prius converter IPM (right).

Figure 2.21 provides a close-up comparison of the power electronics devices of the Camry and Prius boost converter IPMs. The fabrication process for the Camry boost converter IPM is more intricate due to the increased number of devices that need to be interconnected, thereby increasing wire bond count and driver and sensor feedback signals.

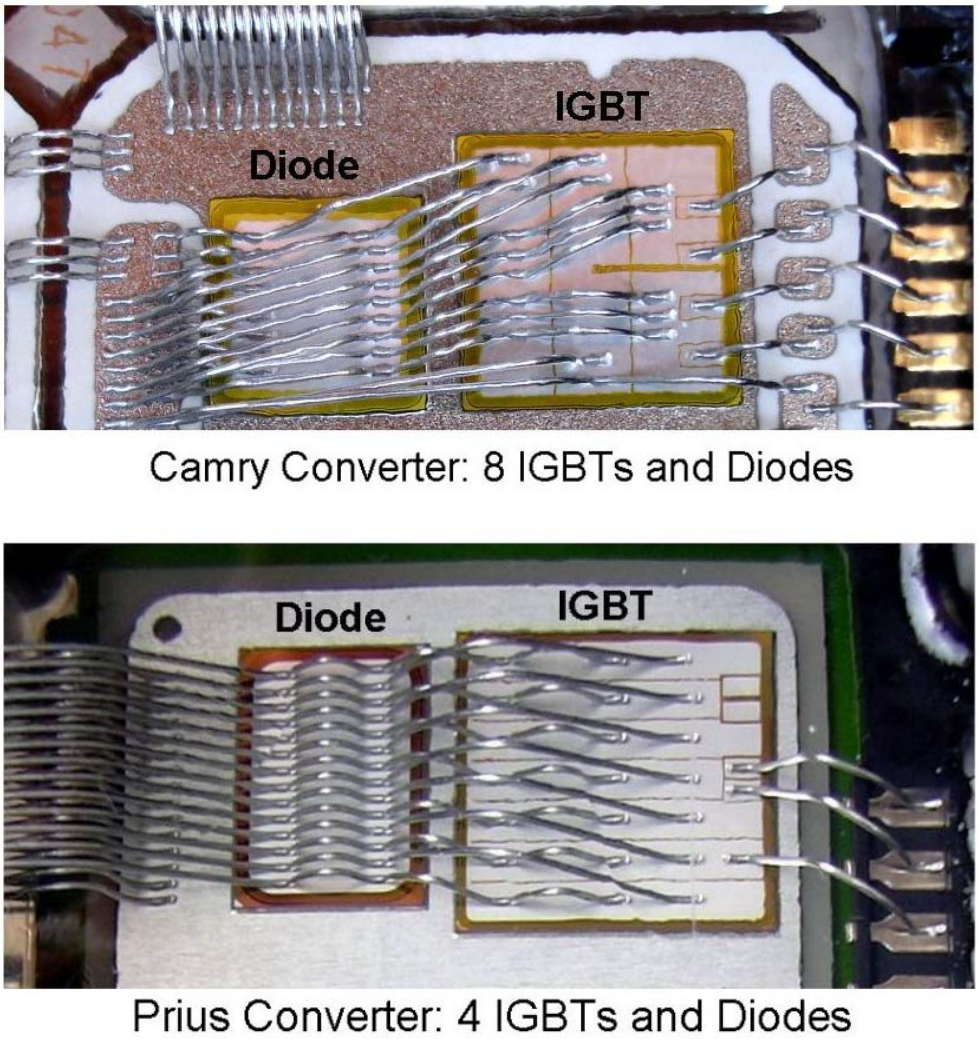

Fig. 2.21. Close-up comparison of Camry converter IPM (upper) and Prius converter IPM (lower).

Table 2.5 summarizes the device count, wire-to-silicon (Si) bond count on the emitter surface, and amount of Si used in the Camry and Prius motor inverters and boost converters. The ratios of heat spreader area to total power electronic device Si area for the Camry motor inverter and boost converter are 10.1 and 4.3, respectively. The smaller ratio suggests a great success in size reduction (i.e., a small heat sink relative to the amount of Si). For comparison, the corresponding ratios for the Prius are 21.7 and 6.8. Again, these improvements are the result of the challenges of implementing the hybrid system into an already existing vehicle, whereas the Prius was strictly designed to be an HEV where volumetric constraints were not as restrictive.

Table 2.5. Summary of power electronic device packaging

Parameter	Motor Inverter		Buck/Boost Converter	
	IGBTs	Diodes	IGBTs	Diodes
Camry				
Number of devices	18	18	8	8
Emitter wire bond count per device.	27	12	18	17
Area of total Si die per device, mm^2.	120.3	71	177	104
Summation of Si area, mm^2.	2165	1278	1400	830
Heat spreader area/Si area.	34800/3443 = 10.1		9530/2230 = 4.3	
Prius (for comparison)				
Number of devices.	12	12	4	4
Emitter wire bond count per device.	20	5	21	28
Area of total Si die per device, mm^2.	131.9	40.7	228	119
Summation of Si area, mm^2.	1583	488	910	475
Heat spreader area/Si area.	45100/2071 = 21.7		9400/1385 = 6.8	

2.1.2 Capacitor Test Results

As capacitor technologies mature, it is important to ascertain the capabilities and limitations of these new technologies by subjecting them to standardized tests to evaluate their characteristics. Test results will assist in benchmarking not only the capabilities and limitations of these technologies, but also to provide a baseline for comparison. All the capacitors studied are of the metallized plastic film type and were manufactured by Matsushita under the Panasonic brand name, except for the large Camry dc-link capacitor which was manufactured by Nichicon. As noted in Section 2.1, the capacitor modules are made up of several sub-capacitors. Tests were conducted upon the entire modules as well as the individual capacitors which were destructively removed from the entire module.

Capacitor tests were conducted both statically and dynamically. The former is a capacitor parameter assessment and the latter is a thermal characteristic assessment. The static test mode does not entail an externally applied dc-bias voltage and ripple current, but uses only signals supplied by an LCR meter. The capacitor parameters that are measured in the static mode are: (1) equivalent series resistance (ESR), (2) dissipation factor (DF), and (3) capacitance value. The capacitor is placed in an environmental chamber and the temperature is cycled through temperatures ranging from -40º to 140 ºC using steps of 20ºC. These three parameters are measured at each temperature step.

The ESR is the real component of the equivalent impedance of the capacitor and corresponds directly with total energy loss which is dissipated as heat during operation. The DF is the ratio of the ESR over the capacitive reactance, which simplifies to ωRC and will be represented as the percentage of real power associated with a particular reactive power component. Both of these parameters were measured during static tests and the results were plotted over a wide frequency and temperature range.

In dynamic tests, a dc-bias voltage and ripple current is applied to the capacitor and the temperature of the capacitor is monitored. When a capacitor is used on a dc bus, the maximum ripple current capability is an important specification. The dynamic test determines the amount of heat generated by the capacitor as a function of ripple current at various ambient temperatures.

2.1.2.1 Static capacitor test results of the 2098 µF dc-link smoothing capacitor module

The data acquisition system (DAQ) consists of a Dell Precision 380 Workstation running LABView 8.5. In the static mode, the instruments used to log data are an Espec environmental chamber and an Agilent 4284 LCR meter. At the beginning of the static thermal cycling tests, after all temperature steps and test frequencies have been entered, the program turns on the environmental chamber and commands a target temperature to the chamber. After the target temperature has been reached and a pre-programmed delay time has been met, the program sends a command to the LCR meter to output the first test frequency and then begins to monitor the ESR from the capacitor under test. When that value is stable, the ESR is recorded and the next parameter is measured and recorded. After the values for ESR, DF, and capacitance are recorded at the first test frequency, the command is given to the LCR meter to output the next test frequency and the monitoring and recording process is repeated. After all data are recorded at all test frequencies, the next temperature step is commanded to the environmental chamber and the process is repeated.

The Camry capacitor module was tested in the static mode from -40 to 140°C over a frequency range of 100 Hz to 30 kHz. ESR, DF, and capacitance was measured and recorded. An interesting fact is observed in Fig. 2.22 as the capacitance approaches infinity beyond 16 kHz. The module can be represented as an RLC circuit with very small resistance and inductance. At high frequencies, even a small parasitic inductance component has a significant influence upon the entire equivalent reactance of the module. There is a certain resonant frequency where the capacitive (negative reactance) effect and inductive (positive reactance) effect are equal, and therefore the total reactance is zero and the imaginary admittance or susceptance is infinite. Thus, the equivalent capacitance approaches infinity as the frequency approaches resonant frequency. Just beyond the resonant frequency, the equivalent reactance is inductive and increases from zero as frequency increases. Figure 2.23 shows that the Prius capacitor module also has a similar effect near 15 kHz. As discussed shortly hereafter in Section 2.1.2.4, additional tests were conducted to investigate this matter further.

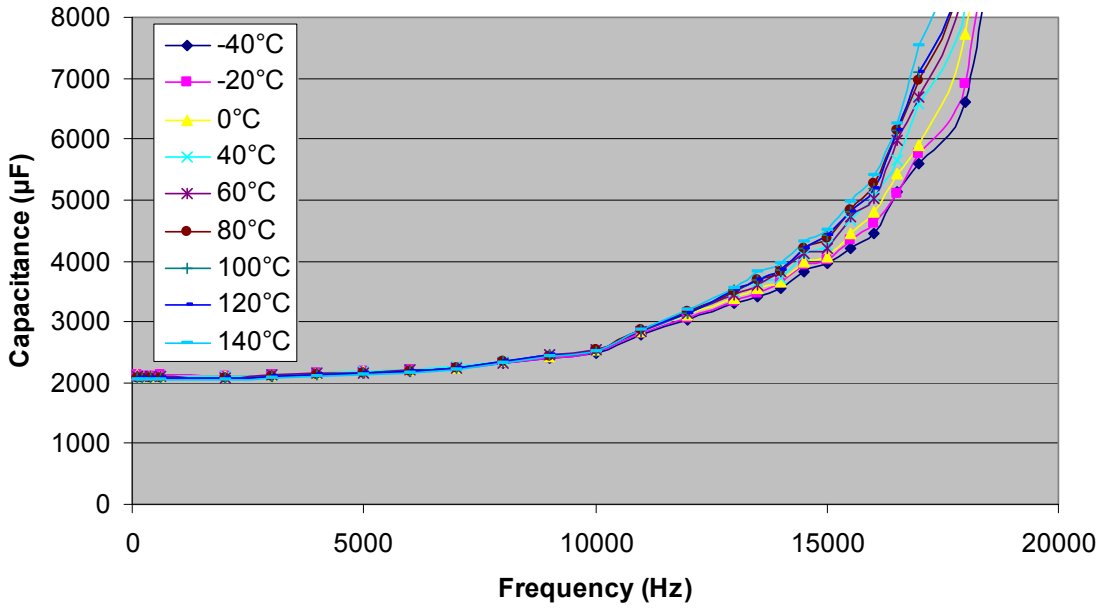

Fig. 2.22. Camry capacitor module equivalent capacitance vs. frequency.

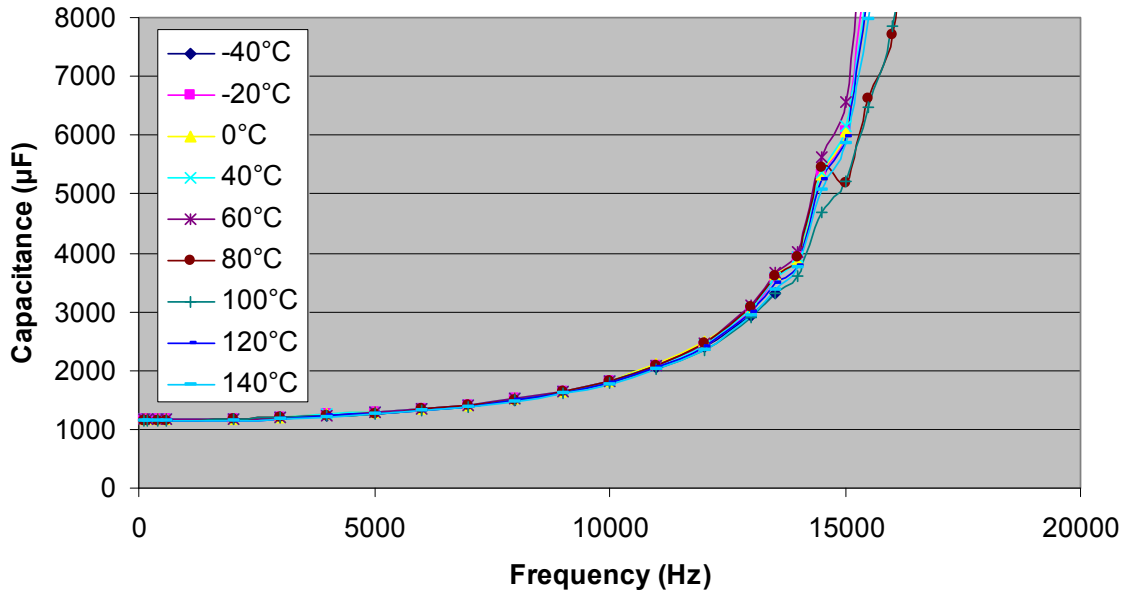

Fig. 2.23. Prius capacitor module equivalent capacitance vs. frequency.

As shown in Fig. 2.24, the response of the entire Camry module capacitance was very minimal over the full temperature range. The largest change in capacitance over the temperature range is observed at 15 kHz, which is also the frequency at which the highest capacitance was measured. For low frequencies, capacitance tended to increase with increasing temperature until peaking at a particular temperature and then the capacitance decreased slightly as temperature increased above this temperature. This peak capacitance temperature increased with increasing frequency. The Prius capacitor module showed similar effect and slight variation of capacitance with temperature.

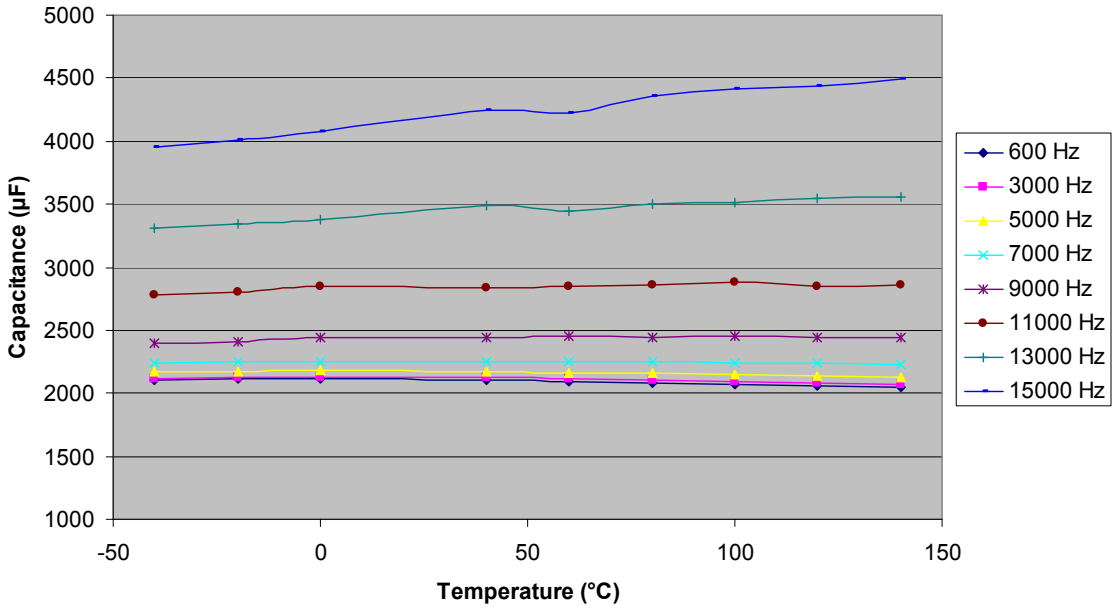

Fig. 2.24. Camry capacitor module equivalent capacitance variation with ambient temperature.

Figures 2.25 and 2.26 show the ESR response to frequency for the Camry and the Prius module, respectively. Although the curve characteristics indicate that the influence of frequency upon the ESR of both modules is reasonably different, the ESR measurement is similar, particularly at low frequencies. Measurements indicate that ESR values generally increased with increasing temperature for both modules at all frequencies.

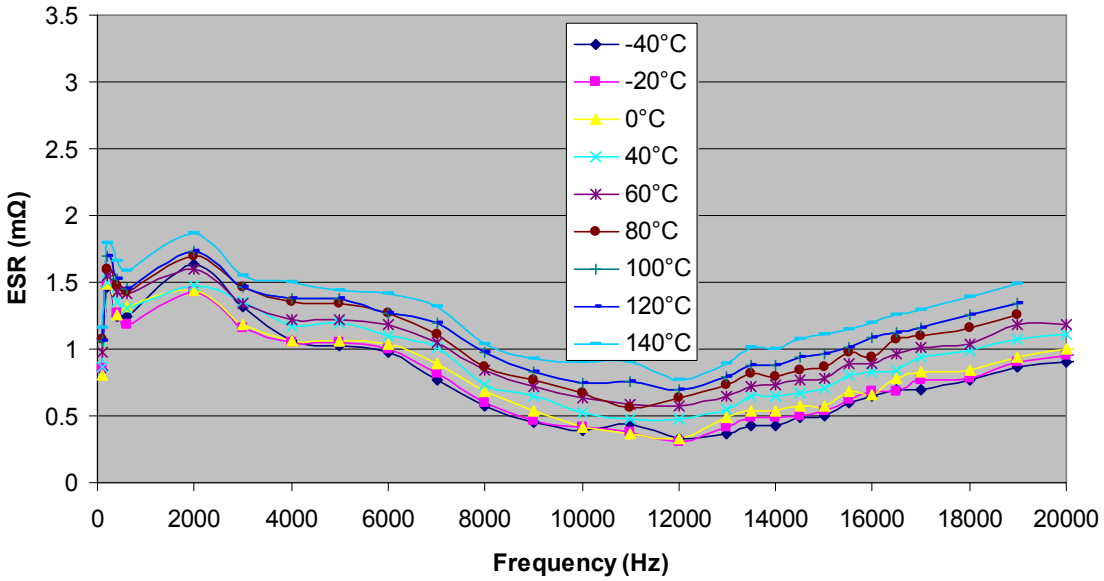

Fig. 2.25. Camry capacitor module ESR vs. frequency.

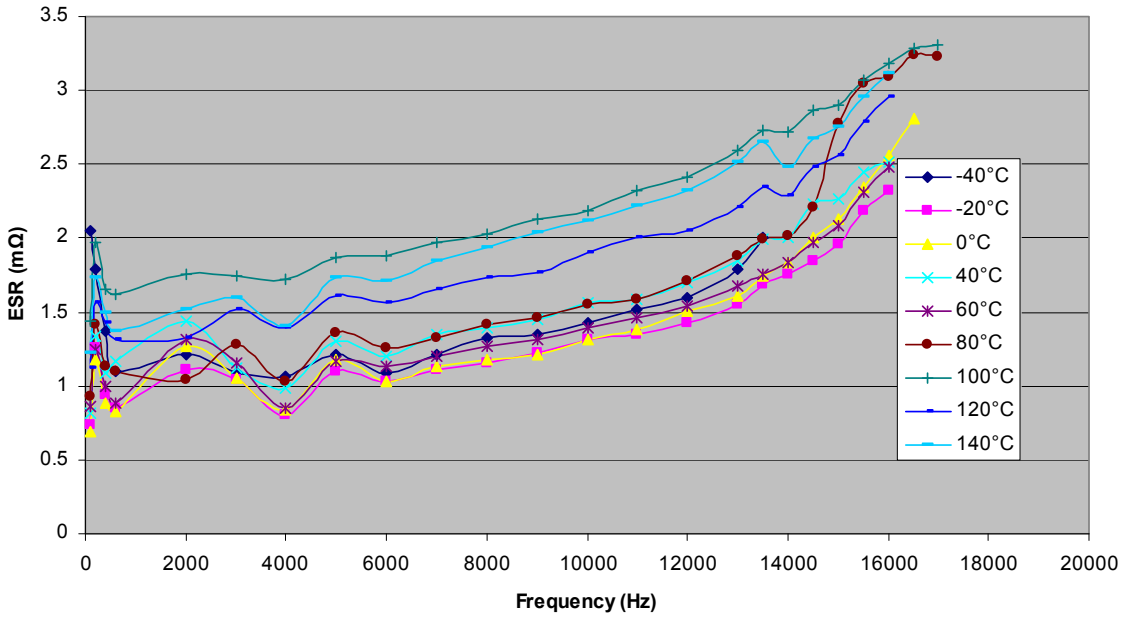

Fig. 2.26. Prius capacitor module ESR vs. frequency.

To obtain a clearer perspective of the impact of temperature upon ESR, Figs. 2.27 and 2.28 shows ESR plotted versus temperature for each frequency for the Camry and the Prius capacitor module, respectively.

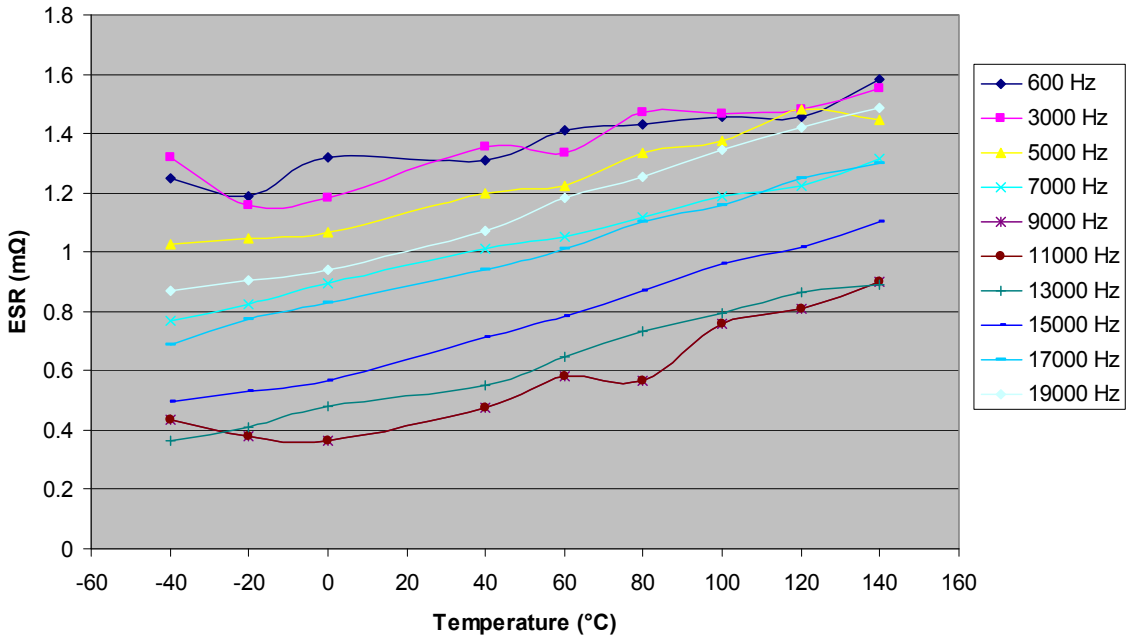

Fig. 2.27. Camry capacitor module ESR vs. temperature.

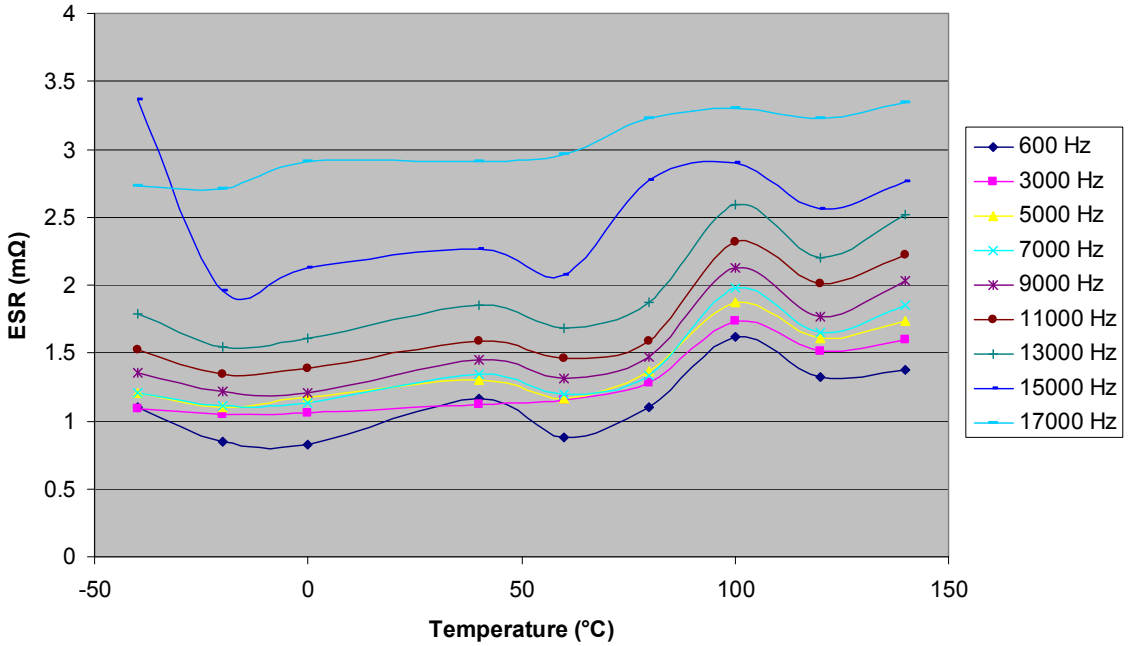

Fig. 2.28. Prius capacitor module ESR vs. temperature.

Again, the ESR of both modules generally increases with increasing temperature. Strangely, the ESR of the Prius module has a substantial lobe at 100°C for all frequencies as well as a high ESR measurement at -40°C and 15 kHz.

The variations of DF with frequency for the Camry and Prius capacitor module are shown in Figs. 2.29 and 2.30, respectively. These graphs are similar to the capacitance versus frequency graphs in Figs. 2.22

and 2.23. Since DF is the product of ESR, capacitance, and frequency, both graphs include curves which approach infinity near the resonant frequency. The behavior of the Camry capacitor module DF as a function of frequency is somewhat peculiar as the frequency increases beyond 6 kHz and then resumes typical behavior beyond about 12 kHz.

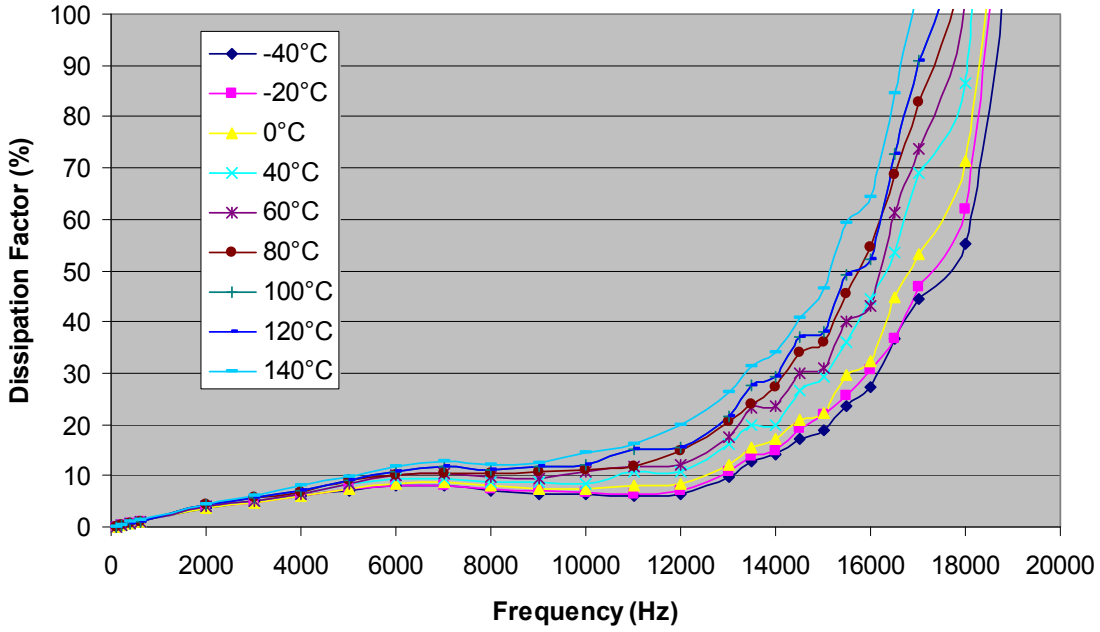

Fig. 2.29. Camry capacitor module DF frequency response.

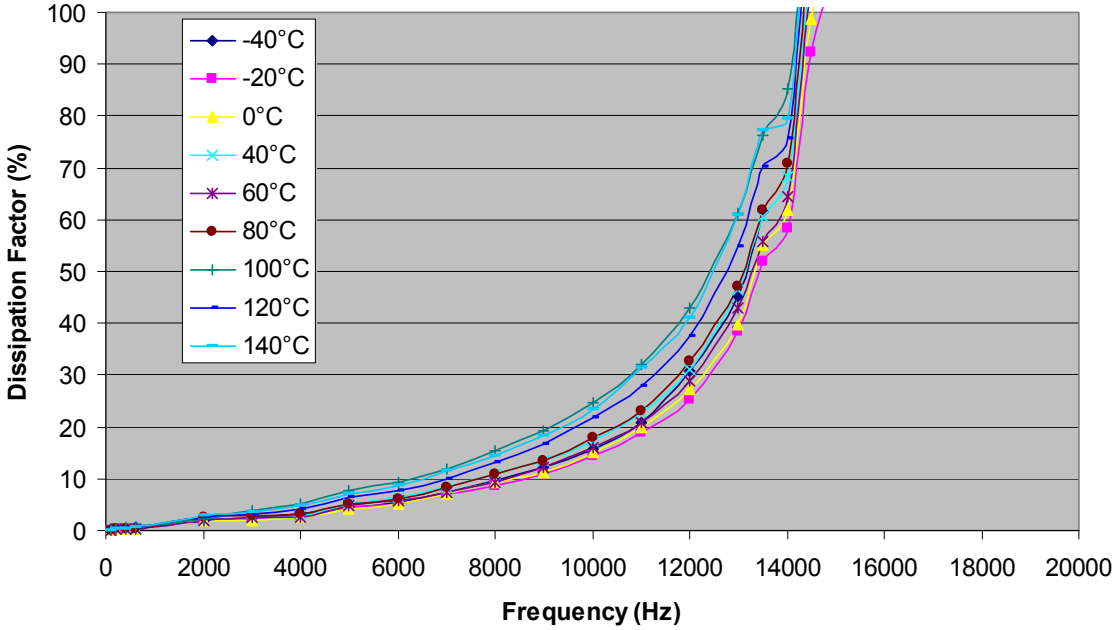

Fig. 2.30. Prius capacitor module DF frequency response.

The impact of temperature on the DF of the Camry and Prius capacitor modules for each test frequency is observed in Figs. 2.31 and 2.32, respectively. Similar to the impact of temperature upon capacitance, the DF generally increases with increasing temperature. Additionally, temperature has a greater impact on DF at higher frequencies. Since the ESR naturally increases with increasing temperature, the amount of real power dissipated at a particular amount of reactive power increases as temperature increases.

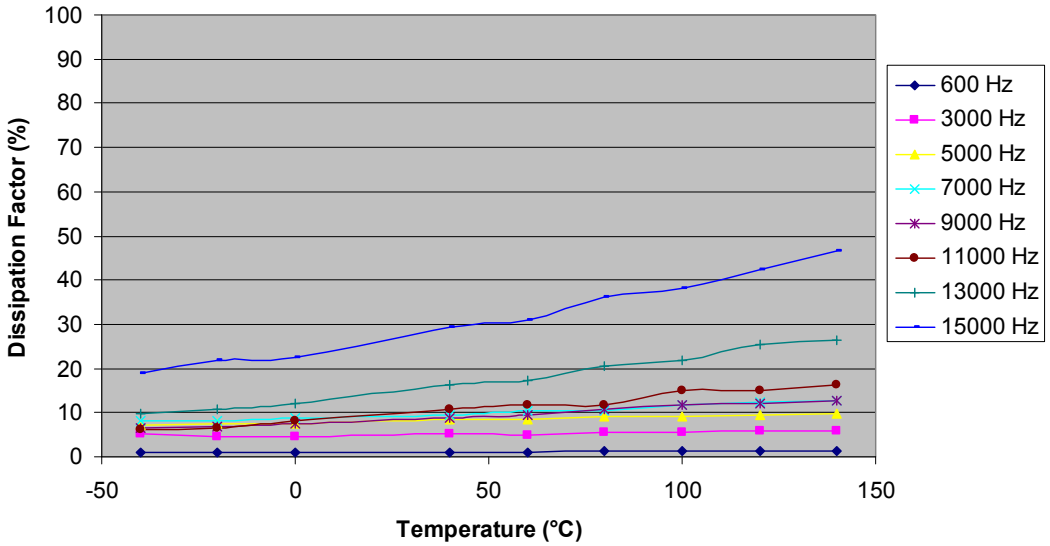

Fig. 2.31. Camry capacitor module DF temperature response.

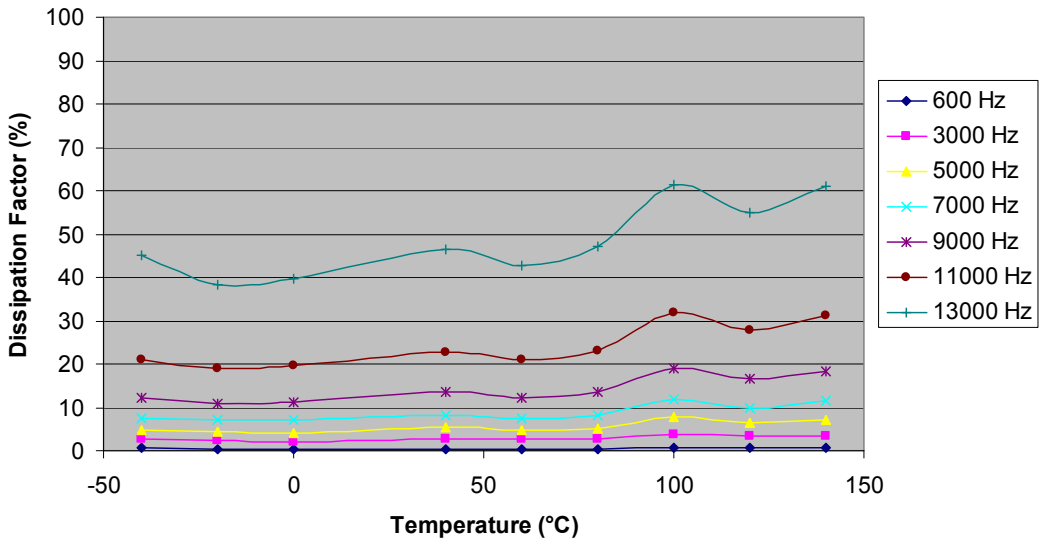

Fig. 2.32. Prius capacitor module DF temperature response.

2.1.2.2 Dynamic capacitor test results from large dc-link capacitor module

The Camry capacitor module was tested with a dc bias of 100 V and a maximum ripple current of 250 A. Figure 2.33 shows the circuit used to apply a ripple current with a dc bias to the capacitor module under